Neuron, Volume *75*

Supplemental Information

Similarity of Visual Selectivity among Clonally Related Neurons in Visual Cortex

Gen Ohtsuki, Megumi Nishiyama, Takashi Yoshida, Tomonari Murakami, Mark Histed, Carlos Lois, and Kenichi Ohki

FigureS1 related to Figure1

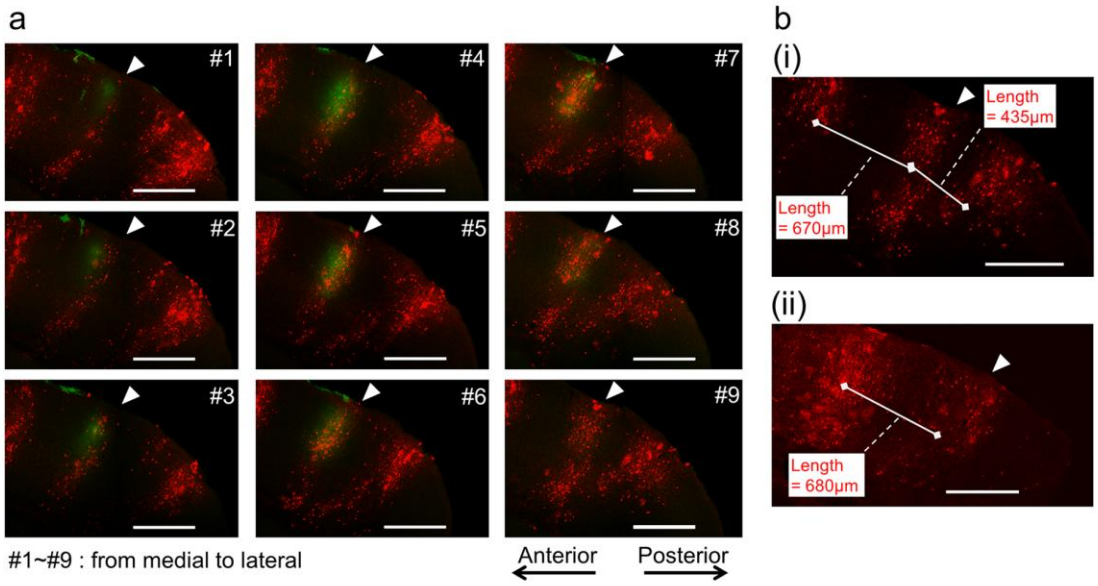

Figure S1 related to Figure 1

Spatial distribution of clonally-related sister cells

a. A series of tangential sections (50 μm) of visual cortex from the Ai9 x TFC.09 transgenic mouse shown in the Figure 1 of the main text. Clonally-related cells were labeled with tdTomato (red). Arrowheads indicate the position of the single clone observed with two-photon microscopy in vivo. Green inside the cortex: Oregon Green BAPTA-1 AM 488 (OGB-1). Green on the cortical surface: FluoSphere used for marking the imaging site. Scale bar indicates 500 μm. Slices were prepared with typical histological methods after calcium imaging, and imaged with confocal microscopy.

b. Distances between clonally-related clusters. **b-(i)**, A tangential section of visual cortex from the mouse shown in **a**. Distances between the targeted cluster and nearest clusters were 435 μm and 670 μm (solid lines). Distances were measured at layer 4, from sequential 4 slices and averaged. **b-(ii)**, Another example of an isolated single cluster from another mouse. Distance from the nearest cluster was 680 μm. Scale bar indicates 500 μm.

Figure S2 related to figure 2

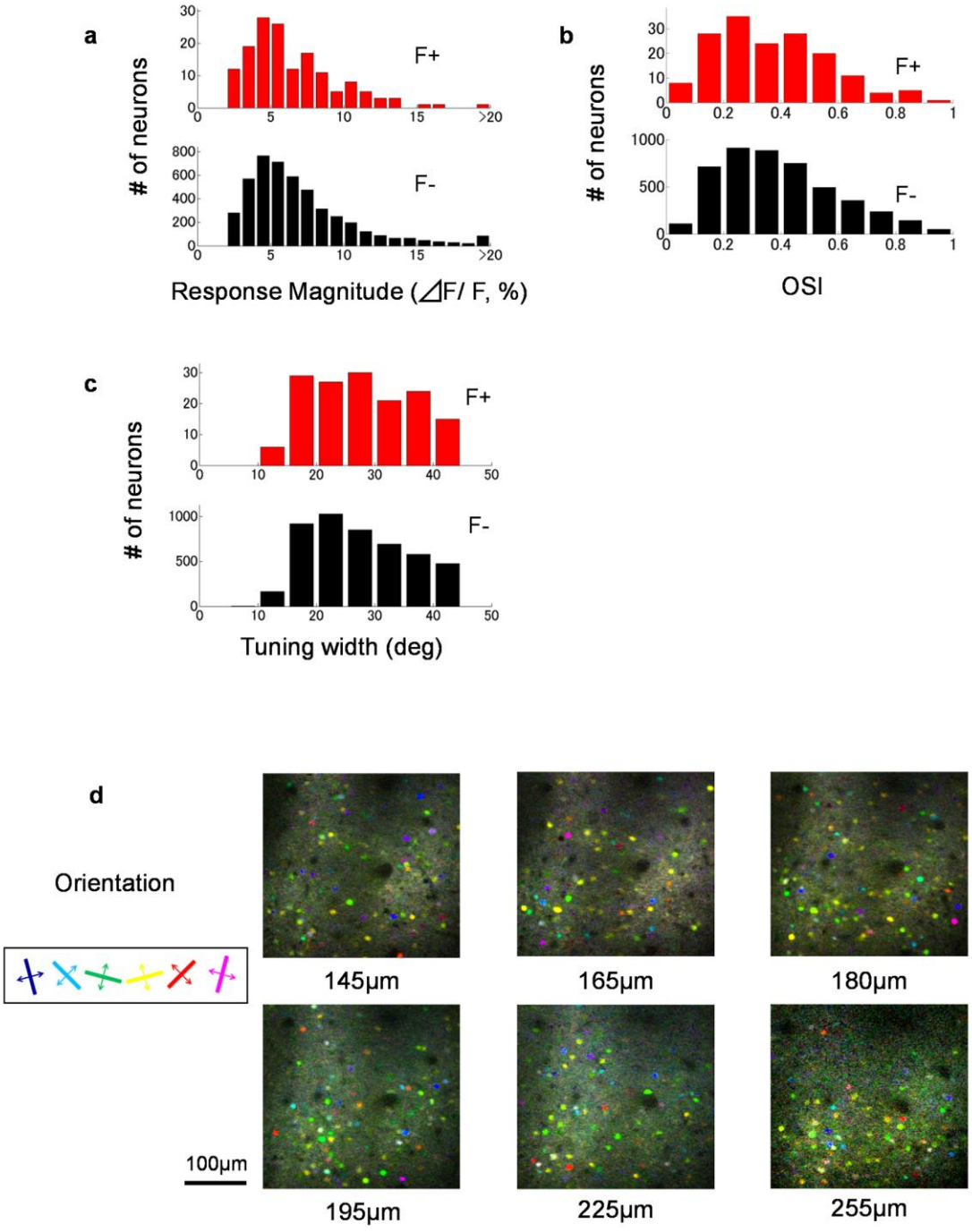

Figure S2 related to Figure2

a-c. Comparisons of visual responsive properties between fluorescently-labeled (F+) and non-labeled cells (F-). Data were collected from 8 imaging sites in 7 transgenic animals (TFC.09 x loxP reporter mice). Both types of cells showed similar properties in maximum response magnitude (**a**), orientation selectivity index (**b**), and tuning width of direction selectivity (**c**) ($p > 0.1$ in all three cases by Kolmogorov-Smirnov (KS) test. 152 F+ and 4726 F- cells). Only visually selective cells were used in these analyses. Visually selective cells were defined by ANOVA ($p < 0.01$) across blank and twelve direction periods, $\Delta F/F > 2\%$, ANOVA ($p < 0.01$) across six orientations, and tuning width < 45 degrees (see Experimental Procedures in the main text).

d. An example of orientation maps in a TFC.09 x loxP reporter mouse with a strong bias in preferred orientation of local neurons (shown in the Figure 3b of the main text). Typical salt-and-pepper orientation maps were observed.

Figure S3 related to figure 3

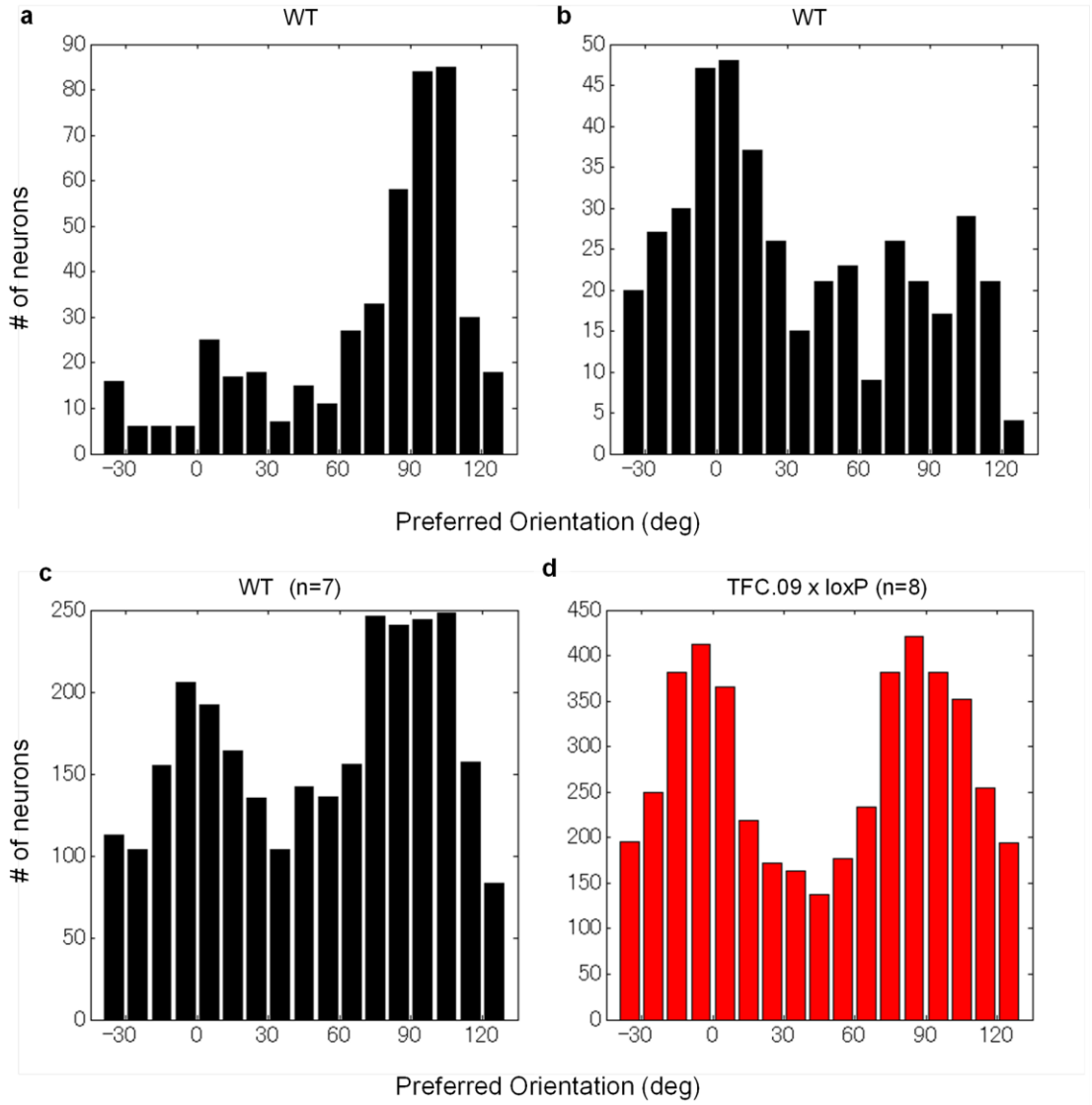

Figure S3 related to Figure 3

Comparison of orientation biases between TFC.09 x loxP reporter mice (TFC.09) and wild-type C57BL/6 mice (WT).

a, b. Histograms of biases in preferred orientation in two WT.

Data were collected from several different planes, and pooled together in each mouse. Biases to horizontal (around 90 degrees in **a**) and vertical bar stimuli (around 0 degree in **b**) were observed. Recording conditions were very similar to those in the main experiments except for mouse lines.

To quantify orientation bias in each mouse, fast Fourier transform was applied to the orientation histogram to compute baseline (F0), first (F1) and second (F2) harmonics. F0 reflects mean value of histogram, and F1 and F2 indicate amplitudes of fitting sine curve with one and two cycles, respectively. Two indexes defined by F1/F0 and F2/F0 were used for the bias evaluation. Both indexes were not significantly different between WT (n = 7) and TFC.09 (n = 8). F1/F0: 0.45 ± 0.22 (mean ± standard deviation) and 0.46 ± 0.27 in WT and TFC.09, respectively ($p > 0.1$ by Kolmogorov-Smirnov (KS) test). F2/F0: 0.42 ± 0.19 and 0.44 ± 0.19 in WT and TFC.09, respectively ($p > 0.1$ by KS test).

c, d. Population histograms of preferred orientation in WT and TFC.09 after pooling histograms from all the examples (n = 7 and 8, respectively).

Supplemental Experimental Procedures

All experiments were carried out in accordance with institutional animal welfare guidelines laid down by the Animal Care and Use Committee of Kyushu University, and approved by the Ethical Committee of Kyushu University.

Transgenic animals

Z/EG (Novak et al., 2000) and Ai9 (Madisen et al., 2010) mice were obtained from the Jackson Laboratory. TFC.09 mice were generated by enhancer trapping, in which the minimal promoter of mouse Thy-1.2 gene regulates Cre recombinase expression (Magavi et al., 2012).

Animal preparation

Mice (postnatal days P49–62) were prepared for in vivo two-photon imaging as previously described (Ohki and Reid, 2011). The anesthesia was induced with isoflurane (3%), and maintained with isoflurane (1–2% in surgery, 0.5–1% during imaging). To prevent dehydration during surgery and recording, the eyes were coated by a thin layer of silicone oil. A small craniotomy was made over the visual cortex, and the underlying cortex was covered with artificial cerebrospinal fluid (ACSF) (150 mM NaCl, 2.5 mM KCl, and 10 mM HEPES [pH 7.4])).

Dye loading and in vivo two-photon imaging

0.8mM OregonGreen 488 BAPTA-1 AM (OGB-1 AM) was dissolved in DMSO with 20% pluronic acid and mixed in ACSF containing 0.01-0.02% Fast Green (all from Molecular Probes). A patch pipette (tip diameter of 3-4 μm) was filled with this solution and inserted into the cortex to a depth of 200–600 μm from the surface. OGB-1 AM and Fast Green were pressure-ejected from the pipette (5–12 p.s.i. for 40–80 s). This enabled to stain a column-shaped volume region of about 400 μm diameter with 650 μm depth at maximum. Full loading of the OGB-1 AM dye by cortical somata took 30 minutes. After confirming loading, the pipette was withdrawn and the craniotomy sealed with a glass coverslip.

Two-photon imaging of changes in calcium fluorescence in cortical cells was monitored with a Zeiss LSM7MP, Nikon A1MP, Leica TCS SP2, or a custom-built scope, and a MaiTai Deep See (Spectra Physics) mode-locked Ti:sapphire laser (920 nm). Excitation light was focused by 25x Olympus (NA: 1.05) or Nikon PlanApo objectives (NA: 1.10). The average power delivered to the brain was < 35mW, depending on depth of the focus. OGB-1 and tdTomato were excited at 920 nm, and eGFP was excited at 960 nm (Kerlin et al., 2010). The emission filters were 432-482 nm for eGFP, 517-567 nm or 470-550 nm for OGB-1, and 600-650 nm for tdTomato.

Visual stimulation and image data acquisition

Drifting square-wave gratings (100% contrast, 1–2 Hz) were presented on a 19-inch LCD monitor at twelve directions of motion in 30 degree steps. Spatial frequency was set at 0.025–0.16 cycles per degree. Each stimulus started with a blank period of uniform grey (4 s) followed by the same period of visual stimulation. In some experiments, we presented two spatial frequencies, for example, 0.04 cycle/deg and 0.10 cycle/deg, for 2 seconds each, during presentation of single orientations (4 seconds). We did not see a significant increase in the number of responsive cells. The twelve orientation stimuli were presented sequentially and repeated ten to twenty times. Care was taken to shield the microscope objective and the photomultipliers from stray light. Images were obtained by Zeiss Zen or Nikon NIS Elements software. A square region of cortex 300-423 μm on each side was imaged at either 256 x 256 or 512 x 512 pixels at 30-200 ms per frame. In all experiments, images were obtained from 130-520 μm depths separated by at least 15 μm. Three-dimensional anatomical reconstruction was obtained by imaging at 2.0-2.5 μm spacing in depth.

Histological reconstruction

The animals were deeply anesthetized with pentobarbital after completing the experiments, and transcardially perfused (phosphate buffered saline, followed by 4% paraformaldehyde, 10% to 30% sucrose). After perfusing the brain, FluoSpheres (Yellow-Green, F8803, Molecular

Probes) was injected into the cortical surface to mark the in vivo imaging site, using the remaining OGB-1 signal as a landmark for injection. The cortex was dehydrated in 30% sucrose for a few days and frozen, and a series of 50 μm sagittal or coronal sections of imaged cortex was cut on a freezing microtome (Microm HM550). Sections were imaged with a Nikon A1Rsi confocal imaging system and Nikon ×10/0.45 numerical aperture objective. Images were captured with NIS Elements (Nikon). OGB-1 and FluoSpheres fluorescence was excited at 488 nm using argon laser (CVI Melles Griot), and imaged at 500-550 nm. TdTomato was excited at 562 nm and imaged at 570-620 nm.

Data analysis

Images were analyzed in Matlab (Mathworks) and ImageJ (National Institutes of Health). Images were realigned by maximizing the correlation between frames. Cells were automatically identified by template matching with a circular template with the size of neural cell bodies. Automatically identified cells were visually inspected and the rare but clear errors were corrected manually. We identified 38,760 cells and 1,049 cells were fluorescently-labeled (F+). Time courses of individual cells were extracted by summing pixel values within cell contours. Slow drift of the baseline signal over minutes was removed by a low-cut filter (Gaussian, cut-off, 1.6 minutes) and high frequency noise was removed by a high-cut filter (1st order Butterworth, cut-off, 1.6 seconds). To minimize neuropil signal contamination, background time course of signal obtained from surrounding part of a cell body was subtracted from the each cell's time course after multiplying a scaling factor (Kerlin et al., 2010). The scaling factor was determined in each field of view by computing ratio of mean fluorescent signal of blood vessel to that of surrounding background signal averaged across several blood vessels. Visually responsive cells were defined by ANOVA ($p < 0.01$) across blank and twelve direction periods and $\Delta F/F > 2\%$ (558 F+ cells and 16,055 F- cells). Of these, selective cells to orientation were defined by ANOVA ($p < 0.01$) across six orientations (270 F+ cells, 6,942 F- cells). Tuning curves of these selective neurons were fit with the sum of two circular Gaussian functions (von Mises distributions) and tuning widths were measured as half-width at half maximum (HWHM). Of

these, sharply selective cells were defined by tuning width < 45 degrees (149 F+ cells and 4,614 F- cells). Preferred orientation was obtained by vector averaging (Swindale et al., 1987). Orientation selectivity index (OSI) was calculated as the magnitude of the vector average divided by the sum of all responses: $OSI = ((\Sigma R(\theta_i)\sin(2\theta_i))^2 + (\Sigma R(\theta_i)\cos(2\theta_i))^2)^{1/2}/\Sigma R(\theta_i)$, where θ_i is the orientation of each stimulus and $R(\theta_i)$ is the response to that stimulus (Worgotter and Eysel, 1987). Kuiper test was performed with a circular statistics toolbox, CircStat (Berens, 2009).

For pixel-based analysis, images were averaged over stimulus repetitions, and spatially smoothed (Gaussian, σ=1 μm). Fluorescence change (ΔF) maps were obtained by subtracting images during the blank period from images during which one of twelve directions was presented. Hue-lightness-saturation (HLS) orientation maps (Fig. 2c) were obtained from these 12 ΔF maps. The hue of each pixel is determined by the best orientation, the color saturation is proportional to the orientation selectivity index (OSI), and the brightness is proportional to the fluorescence change (ΔF) to the best orientation.

Bootstrap analysis

We used a bootstrap to confirm that neither the bias in the preferred orientations of the F- cells or possible spatial clustering of F+ cells did not artifactually cause the statistical difference. On each bootstrap repetition, for each sharply selective F+ cell, a sharply selective F- cell was chosen randomly within a 50 micron radius. In this way we obtained a set of randomly chosen sharply selective F- cells that were matched in number and spatial location to the sharply selective F+ cells. The distribution of these randomly chosen F- cells was compared with the entire set of F- cells with a Kuiper test across a wide range of p-values. Any significant difference is a false positive. 100,000 repetitions were simulated for each p-value and for each clone, and false positive rates were obtained.

We compared the differences in preferred orientations (ΔOri) of all the possible pairs among F+ cells and the ΔOri of all the possible pairs between F+ and F- cells. Again, a bootstrap was

used to correct the p-values obtained from the Kolmogorov-Smirnov test.. We obtained a set of randomly chosen sharply selective F- cells, matched in number and spatial location to the sharply selective F+ cells, in the same way as described above. By comparing differences of ΔOri among this population and ΔOri between this population and the entire F- population using a Kolmogorov-Smirnov test, false positive rates were obtained across a wide range of p-values. The p-value was corrected with the false positive rate obtained from the bootstrap at a p-value threshold obtained by comparing actual clonally-related and non-related pairs.

Supplemental References

Berens, P. (2009). CircStat: A Matlab Toolbox for Circular Statistics. Journal of Statistical Software, 31 (10) 1-21.

Worgotter, F., and Eysel, U.T. (1987). Quantitative determination of orientational and directional components in the response of visual cortical cells to moving stimuli. Biol. Cybern. 57, 349-355.